Brigham Young University
BYU ScholarsArchive

All Theses and Dissertations

2018-06-01

Mercury and Dissolved Organic Matter Dynamics During Snowmelt in a Montane Watershed, Provo River, Utah.

Brian Noel Packer
Brigham Young University

Follow this and additional works at: https://scholarsarchive.byu.edu/etd

 Part of the Physical Sciences and Mathematics Commons

BYU ScholarsArchive Citation

Packer, Brian Noel, "Mercury and Dissolved Organic Matter Dynamics During Snowmelt in a Montane Watershed, Provo River, Utah." (2018). *All Theses and Dissertations*. 7427.
https://scholarsarchive.byu.edu/etd/7427

This Thesis is brought to you for free and open access by BYU ScholarsArchive. It has been accepted for inclusion in All Theses and Dissertations by an authorized administrator of BYU ScholarsArchive. For more information, please contact scholarsarchive@byu.edu, ellen_amatangelo@byu.edu.

www.manaraa.com

Mercury and Dissolved Organic Matter Dynamics

During Snowmelt in a Montane Watershed,

Provo River, Utah

Brian Noel Packer

A thesis submitted to the faculty of
Brigham Young University
in partial fulfillment of the requirements for the degree of

Master of Science

Gregory T. Carling, Chair
Stephen T. Nelson
Zachary T. Aanderud

Department of Geological Sciences

Brigham Young University

Copyright © 2018 Brian Noel Packer

All Rights Reserved

www.manaraa.com

ABSTRACT

Mercury and Dissolved Organic Matter Dynamics
During Snowmelt in a Montane Watershed,
Provo River, Utah

Brian Noel Packer
Department of Geological Sciences, BYU
Master of Science

Mercury (Hg) transport in streams is typically facilitated by dissolved organic matter (DOM), however, the dynamics of Hg and DOM during snowmelt in montane watersheds are poorly understood. Hg transport during snowmelt is widely recognized as a significant source of Hg to downstream lakes and reservoirs, such as Jordanelle Reservoir where fish consumption advisories are in effect due to elevated Hg concentrations in certain species of fish. For this study, total mercury (THg), methylmercury (MeHg), and DOM samples were collected at three sites in the upper Provo River, northern Utah, during the 2016 and 2017 water years. To evaluate Hg and DOM sources, samples were collected from snowpack and ephemeral streams in the watershed. In-situ fluorescent DOM (fDOM) data and other parameters were measured in the river to characterize high-frequency variation in water chemistry. Excitation-emissions matrices (EEMs) were used to determine changes in DOM characteristics during snowmelt. Hg concentrations increased in the upper Provo River from <1 ng/L during baseflow to >7 ng/L during the snowmelt period (~April-July), with filtered THg concentrations approximately ~75% of the unfiltered concentrations. In the watershed, filtered THg concentrations ranged from ~0.4 ng/L in snowpack to ~8 ng/L in ephemeral streams. Annual THg loading from the Provo River to Jordanelle Reservoir was approximately 1 kg/yr with ~90% of the flux occurring during the snowmelt period. High correlations between filtered THg and fDOM allowed for the development of a high frequency filtered THg proxy using in-situ fDOM sensors. DOM characteristic during the snowmelt period showed that Hg transport was facilitated by humic substances which was sourced from upland soils. Fractions of filtered methylmercury (MeHg) and filtered THg (filtered MeHG:filtered THg) were ~0.1 during baseflow and reduced to ~0.01 during snowmelt, implying that snowmelt runoff has little impact on the MeHg flux to Jordanelle Reservoir. The results suggest that Hg and DOM are flushed from soils during snowmelt, and that a significant majority of the Hg flux occurs the snowmelt period. Our study has implications for understanding Hg sources and transport mechanisms in other snowmelt dominated watersheds.

Keywords: Mercury, dissolved organic matter (DOM), fluorescent DOM (fDOM), snowmelt, ephemeral streams

www.manaraa.com

ACKNOWLEDGMENTS

I would like to thank my thesis committee Dr. Gregory Carling, Dr. Stephen Nelson, and Dr. Zachary Aaderud for all their knowledge and guidance in this process. I would like to thank Hannah Checketts, Colin Hale, and Natalie Shepherd Barkdull for their help with field and laboratory work. Finally, I would like to thank my parents and sibling for their encouragement and support throughout all my years in school.

www.manaraa.com

TABLE OF CONTENTS

www.manaraa.com

LIST OF TABLES

www.manaraa.com

LIST OF FIGURES

www.manaraa.com

1. Introduction

Flushing and erosion of the soil surface mobilizes and transports mercury (Hg) to streams during snowmelt. In montane watersheds, the snowmelt period often accounts for the majority of annual Hg export (Mast et al., 2005). Atmospheric Hg deposition, which has tripled since the industrial revolution, is a significant source of Hg in the terrestrial landscape and aquatic systems (Streets et al., 2011), even in remote watersheds (Lucotte et al., 1995). Atmospheric Hg deposition rates can be enhanced in montane watersheds due to high precipitation rates and processes such as cold condensation (Schroeder and Munthe, 1998). Atmospherically deposited Hg in soils and other surfaces is mobilized and transported to streams during high flow events. In streams, Hg typically remains mobile until it reaches a larger water body (Bank, 2012b). Hg transport is facilitated by particulate organic matter (POM) or dissolved organic matter (DOM) (Bank, 2012a). Although DOM and Hg are often correlated, the mechanisms of Hg-DOM binding are poorly understood (Ravichandran, 2004).

Hg can be transformed to the more harmful form of methylmercury (MeHg) in terrestrial and aquatic systems. MeHg is a potent neurotoxin of serious concern to human development and health (Mergler et al., 2007). The methylation of Hg to form MeHg is a biologically mediated process primarily dominated by sulfate and iron reducing bacteria (Ullrich et al., 2001). Wetlands and anoxic lake sediments are important environments where methylation processes can occur (Paranjape and Hall, 2017). Several studies have suggested that methylation can occur in soils during the snowmelt period, and could be an important for studying the Hg budget of a snow dominated watershed (Haynes et al., 2017; Lehnherr et al., 2012). MeHg bioaccumulates up the food web from microbial organisms to increasingly predatory organisms, particularly fish.

www.manaraa.com

The bioaccumulative properties of MeHg can produce fish with tissue concentrations of Hg in parts per million, even if concentrations in the water are in parts per trillion (Morel et al., 1998).

The slope (b) of a log-log concentration-discharge (C-Q) relationship can be used to determine hydrologic behaviors of Hg and other trace metals such as flushing (b>1), chemostasis (b=1), or dilution (b<1). The hydrologic behavior of trace metals gives insight to flow paths taken by the trace metals during high flow events such as snowmelt (Winnick et al., 2017). Hysteresis in C-Q relationships occurs when there is a difference in the relative timing of solute and discharge responses (Evans and Davies, 1998). A clockwise hysteresis occurs when the solute peaks before maximum discharge, and a counter-clockwise hysteresis is when the solute peaks after maximum discharge. Combing C-Q relationships with DOM analysis provides a more detailed understanding on the mechanisms governing the mobilization and transport of certain trace metals such as Hg (Rue et al., 2017).

DOM is an important constituent of soils and surface waters, and fundamental to understanding transport of trace metals such as Hg. Typically, measurements of bulk dissolved organic carbon (DOC) are used to explain DOM cycling and trace metal interactions. However, the biochemical composition of DOM can significantly affect Hg transport in a watershed (Ravichandran, 2004). Fluorescence spectroscopy can shed new light on DOM characterization in freshwater environments, providing insight to the mechanisms governing Hg transport in freshwater ecosystems (Lu and Jaffe, 2001). DOM can be made of many components including humic, fulvic, and protein like substances (Xie et al., 2017). Because of strong relationships between DOM and Hg, in situ measurements of fluorescent DOM (fDOM) can be used as a proxy for filtered THg concentrations. This allows for high frequency filtered THg data to be available where fDOM sensors are installed (Bergamaschi et al., 2012). Measurements for

www.manaraa.com

fDOM are in quinine sulfate units (QSU), and is defined as 1 QSU = 1 ppb quinine sulfate (Chepyzhenko and Chepyzhenko, 2017).

The purpose of this study is to evaluate mechanisms of Hg transport during snowmelt in a montane watershed. Specific objectives are to: 1) investigate concentration-discharge relationships for Hg and DOM; 2) evaluate the sources of Hg and DOM at the watershed-scale; 3) develop high-frequency Hg datasets using fDOM as a proxy for Hg; 4) quantify Hg loads and fraction of dissolved versus particulate Hg; and 5) examine MeHg inputs to the river during snowmelt.

The upper Provo River watershed was selected for this study because it is a relatively pristine snowmelt-dominated montane watershed with a comprehensive network of instruments. The watershed is intensively studied as part of the innovative Urban Transitions and Aridregion Hydro-sustainability (iUTAH) project, which has installed aquatic stations in addition to existing USGS stream gages along the Provo River. The upper Provo River watershed is also monitored for precipitation by the NRCS through snow telemetry (SNOTEL) stations. This study is significant because the Provo River provides drinking water to over 65% of Utah's population, and fills Jordanelle Reservoir which has fish consumption advisories for Brown Trout and Smallmouth Bass due to elevated Hg concentrations (https://deq.utah.gov/fish-advisories/waterbody-utah-fish-advisories#jordanelle).

2. Methods

2.1 Study Area

The upper Provo River watershed covers 675 km^2 in the southwestern Uinta Mountains, and is part of the Middle Rocky Mountains physiographic province. The Provo River also

www.manaraa.com

receives diverted water from the Weber River watershed (589 km^2) and Duchesne River watershed (104 km^2) (Fig. 1). The watershed extends from the sub-alpine region around the headwaters of the Provo River to the semi-arid foothills at Jordanelle Reservoir (Woods et al., 2001). Dominant vegetation in the mid to high-elevations regions of the watershed includes lodgepole pine and douglas fir (Lowry et al., 2005). The semi-arid regions at lower elevations are dominated by sedge and sage brush with minor agricultural use along the river. The length of the upper Provo River is ~50 km with a vertical relief of ~1120 m, from ~3000 m asl at the headwaters, to ~1880 m at Jordanelle Reservoir.

The geology in the upper part of the watershed consists primarily of interbedded metasedimentary rocks overlain by surficial glacial deposits and other Quaternary deposits. The lower part of the watershed is dominated by Paleozoic carbonate and Tertiary volcanic rocks (Fig. 1). Shallow, weakly developed soils with a thin loess cap cover much of the upland regions of the watershed (Munroe, 2012).

2.2 Sample collection and preparation for river, ephemeral streams, and snow

River, ephemeral stream, and snow samples were collected from the upper Provo river watershed during the 2016 and 2017 water years (Fig. 1). Over 100 river samples were collected at three locations including Soapstone, Woodland, and Hailstone. We sampled over a range of stream discharge conditions, with increased sampling frequency during the snowmelt runoff period (April - June). 22 ephemeral stream samples were collected during the 2016 and 2017 water years. Ephemeral stream flow occurred in a brief 1-2 month period during snowmelt and likely represents soil water. Ephemeral stream samples were selected by finding locations where active channels were flowing. 26 snow samples were collected from three locations which were representative of the upper watershed (Fig. 1).

www.manaraa.com

For both river and ephemeral streams, samples were collected for unfiltered THg, filtered THg, and DOM. Unfiltered and filtered THg samples were collected in double-bagged Milli-Q rinsed 250 mL FLPE bottles. Filtered THg samples were filtered upon returning to the lab using syringe and 0.45 µm PES filters. Both unfiltered and filtered THg samples were preserved by acidifying to 1% v/v with trace meatal grade HCl. DOM samples were filtered on site using a peristaltic pump and ashed 0.45 µm glass microfiber filters, and collected into ashed 60 mL amber glass vials. During each sampling day a field blank of Milli-Q water was taken for each sample type as a quality control for contamination. Samples were collected in accordance to 'clean hands, dirty hands' method established by the EPA to prevent contamination (USEPA, 1996).

Snow samples were collected to evaluate atmospheric deposition of Hg to winter snowpack. Snow samples were collected at peak snowpack (mid-April) during 2017 and 2017 in accordance to Carling et al. (2012) by digging the three snow pits at each site to within 10 cm of the ground. Temperature and visual observations of each snow pit were taken in 10 cm increments and recorded in a field notebook. Using acid washed acrylic tubes measuring 45.5cm x 5.5 cm, snow cores were transferred into acid washed 2.5 L FLPE bottles and then double bagged. A field blank of Milli-Q water was collected at each sampling site to ensure no contamination occurred during the collection process. Snow samples were collected in accordance to 'clean hands, dirty hands' method established by the EPA to prevent contamination (USEPA, 1996). In the lab, snow samples were melted and aliquots were taken for measurements of unfiltered THg, filtered THg, and DOM.

2.3 THg and DOM Laboratory analysis

www.manaraa.com

Filtered and unfiltered THg samples were prepared according to EPA Method 1631 and analyzed on the Brooks Rand Merx-T system (USEPA, 2002). As a quality control a 1-5 ng/L matrix spikes were made at least every 10 samples. Filtered and unfiltered MeHg samples were prepared by direct ethylation and analyzed on the Brooks Rand Merx-M system (Mansfield and Black, 2015). As a quality control a 1 ng/L matrix spike was made for every sample. Detection limits were 0.02 ng/L for THg and 0.002 ng/L for MeHg. For both THg and MeHg the "dissolved" fraction was designated as the filtered (0.45 μm) portion of the analysis. The difference between the unfiltered and filtered THg is the particulate fraction of THg (unfiltered Hg – filtered Hg = particulate Hg)

DOM samples were analyzed by measuring the absorbance spectra and fluorescence excitation-emissions matrix (EEM) using the Horiba Scientific AQUALOG. Excitation and emission values from the DOM analysis were then processed through MATLAB to determine the organic matter type along with the fluorescence and freshness indices (Stedmon and Bro, 2008). The fluorescence index indicates if DOM is more microbial (FI ~ 1.8) in nature or more terrestrial (FI ~ 1.2). It is calculated by dividing the 380 nm emission by the max emission intensity between 420-435 nm at an excitation of 310 nm. The freshness index (BIX) indicates the proportion of recently produced DOM (microbial) over older DOM (decomposition of organic matter) (Gabor et al., 2014). DOM characteristics are only available for the 2017 water year due to technical issues involving samples from the 2016 water year.

2.4 Quantifying THg loads from concentration and discharge data

Daily, seasonal, and yearly loads for unfiltered and filtered THg were estimated using the LOAD ESTimator (LOADEST) program from the USGS (Runkel et al., 2004). Loads were calculated using THg concentrations of river samples and discharge measurements from iUTAH

www.manaraa.com

and USGS stations. Load values of µg/day were calculated each hour for every day that had available discharge data. The mean of the 24 hourly load values during each day was used as the daily load. Standard error options were set calculate the exact standard error for the adjusted maximum likelihood estimation of load, and the program was set to select the best regression model to describe C-Q relationships. No discharge data was available during certain times of the year such as when the river was frozen or when the Woodland station was washed away during 2017 snowmelt runoff. Load values when the river was frozen were assumed to be similar to loads during other baseflow conditions. THg loads at Hailstone represent the flux of THg entering Jordanelle Reservoir from the upper Provo River.

3. Results

3.1 Stream discharge and THg concentration response to snowmelt

THg concentrations were associated with discharge at Soapstone, Woodland, and Hailstone during the 2016 and 2017 water years. The associations were strongest at Hailstone with the peaks occurring at the same time, and weaker at Soapstone and Woodland due to the difference in timing of discharge and THg peaks. THg concentrations increased ten-fold from baseflow to snowmelt periods at all three sites. Highest measured unfiltered THg concentrations during the two water years were 7.8 ng/L (2016) and 8.2 ng/L (2017). During both water years, the hydrographs at all three sites peaked between late May and early June. Peak concentrations for THg occurred on the rising limb of the hydrograph for Soapstone and Woodland, with Soapstone peaking earlier than Woodland. At Hailstone, the THg concentration peaked near the same time as the hydrograph peak for both water years (Fig. 2). Average THg concentrations at baseflow for the three sites was ~1 ng/L during both water years. Filtered THg comprised a

www.manaraa.com

significant portion of the unfiltered THg, with contributions between 52-79%, and the percentage of filtered THg decreasing downstream. Due to filtered THg being the most dominant fraction, it is used primarily to explain all the variations of THg in relationship to discharge.

Comparison of the 2016 and 2017 water years is of interest because of the difference in snowpack. 2016 was a moderately low snowpack year with a SWE of 59 cm (91% of average), and 2017 was a high snowpack year with a SWE of 114 cm (179% of average). Snowmelt discharge response for the two years was between April 1-Jun 10 (2016) and March 15-July 31 (2017).

3.2 Filtered THg concentration discharge and hysteresis

Filtered THg concentration-discharge (C-Q) plots showed flushing behavior during the snowmelt period (Fig. 3). For all three locations, and for both water years, filtered THg increased by at least one order of magnitude in response to discharge. At Soapstone and Woodland, filtered THg concentrations increased greatest at discharges between 1-20 m^3/s. After reaching 20 m^3/s the C-Q slope for Soapstone and Woodland became slightly negative ($b<1$). The log-log C-Q plot for Hailstone remained positive ($b>1$) during the entire range of discharge values.

Spatial differences occurred in the characteristics of C-Q hysteresis loops for filtered THg in the upper Provo River (Fig. 4). At Soapstone and Woodland, the hysteresis loops were clockwise, convex, and positively trending (Evans and Davies, 1998). The hysteresis loop of Woodland had a less pronounced clockwise trend compared to Soapstone. At Hailstone, the hysteresis loop showed a more complex figure-eight trend, with the filtered THg concentrations of the falling limb crossing over the rising limb at a discharge 20 m^3/s (Fig. 4).

www.manaraa.com

3.3 DOM characteristics and variability

DOM characteristics varied temporally and spatially during snowmelt in the upper Provo River. EMMs plots during snowmelt showed signatures for humic substances in ephemeral streams and the upper Provo River (Fig. 5). FI decreased during snowmelt at Soapstone, Woodland, and Hailstone (Fig. 6). The highest FI was ~1.65 and occurred at Soapstone during baseflow. The lowest FI of ~1.35 occurred at Hailstone during peak runoff. FI during snowmelt was lowest in ephemeral streams with an average index value of ~1.44. FI values increased downstream with the average FI at Soapstone, Woodland, and Hailstone during snowmelt being 1.46, 1.50, and 1.52 respectively (Fig. 7). There was slight variability in the BIX during the snowmelt Soapstone, Woodland, and Hailstone (Fig. 8). A slight decrease in the BIX occurred at all river sites during snowmelt, followed by an increase after peak snowmelt discharge. Variability in the BIX was minimal between sites, ranging from ~0.5 to ~ 0.75 of recently produced DOM.

3.4 THg loads during the snowmelt season

THg loads were strongly dependent on total discharge during both water years. Estimated daily THg loads for Soapstone, Woodland, and Hailstone during the 2016 and 2017 water years reached as high as 0.05 µg/day during snowmelt runoff (Fig. 9). Loads during baseflow were extremely low, averaging <0.001 µg/day. The snowmelt period of both water years accounted for nearly all of the annual THg flux (88-98%) in the upper Provo River (Table 1). Unfiltered THg loads for Soapstone, Woodland, and Hailstone during the 2016 snowmelt period where 0.64 kg, 0.94 kg, and 0.70 kg respectively. For the 2017 snowmelt period, those loads were 0.82 kg, 1.30 kg, and 1.28 kg. From the 2016 and 2017 water year data, the average annual unfiltered THg yield at Hailstone was estimated at 1 kg/yr, which represents the total flux of THg to Jordanelle

www.manaraa.com

Reservoir. Filtered THg accounted for approximately 56% of the yearly THg load entering Jordanelle Reservoir.

The total load of Hg in snow was comparable to the Hg load in the upper Provo River during snowmelt (Table 1). During the 2016 water year, which had a SWE of 0.59 m, the mass of THg in the upper Provo River watershed was calculated to be ~ 0.66 kg. During the 2017 water year, which had a SWE of 1.14 m, the mass of THg was calculated at ~1.28 kg. For both the 2016 and 2017 water years the estimated mass of Hg in snowpack was >94% of the total Hg flux in the watershed.

3.5 Hg and fDOM relationships

Filtered THg and fDOM (QSU) measurements showed a strong positive correlation at Soapstone ($R^2 = 0.91$) and Woodland ($R^2 = 0.77$) (Fig. 10). The correlation of fDOM to filtered THg at Soapstone and Woodland are described by polynomial equations with x = QSU and y = ng/L of filtered THg. For Soapstone, the equation is $y = 4.58E\text{-}04x^2 + 4.51E\text{-}03x + 5.83E\text{-}01$. At Woodland, the equation is $y = 5.67E\text{-}04x^2 - 1.60E\text{-}02x + 0.601$ *(Fig. 10)*.

Using the polynomial equations, QSU values were used as a proxy to predict filtered THg concentrations (Fig. 11). This proxy allowed for the creation of a high-frequency (fifteen-minute) filtered THg data, which could provide concentration estimates at any time so long and the instrument was collecting data. In both the Soapstone and Woodland dataset there are periods of time when the fDOM sensor was offline, leaving large gaps in the predicted filtered THg values.

3.6 THg concentration variability in snow and ephemeral streams

THg concentrations in snowpack and ephemeral streams were compared with concentrations in the Provo River to evaluate potential Hg sources (Fig. 12).THg concentrations

www.manaraa.com

in snow were significantly lower than concentrations in the upper Provo River during snowmelt. Average unfiltered THg concentrations in snow were 1.5 (2016 water year) and 1.9 ng/L (2017 water year). Average filtered THg concentrations were 0.38 (2016 water year) and 0.32 ng/L (2017 water year). The majority of the THg in snow (79%) for the two water years was in the form of particulate Hg. Compared to Soapstone samples during snowmelt runoff, unfiltered THg concentrations in snow were 106% lower and filtered THg concentrations were 168 % lower.

THg concretions in ephemeral stream were higher than concentrations in the upper Provo River during the 2016 and 2017 snowmelt period. Average unfiltered THg concentrations in ephemeral streams were 9.2 (2016 water year) and 7.8 ng/L (2017 water year). Average filtered THg concentrations were 8.4 (2016 water year) and 7.3 ng/L (2017 water year). The majority of the THg in ephemeral stream (84%) for the two water years was in the filtered fraction. Compared to Soapstone samples during snowmelt runoff, unfiltered THg concentrations in ephemeral streams were 41% higher and filtered THg concentrations were 67% higher.

3.7 Variability in the MeHg:THg ratio

The fraction of filtered MeHg:filtered THg shows and inverse relationship to discharge at Soapstone, Woodland, and Hailstone (Fig. 13). At baseflow, the fraction increased upstream to downstream from ~0.03 at Soapstone to ~0.10 at Hailstone. During snowmelt runoff, the fraction of filtered MeHg:filtered THg decreased to ~0.010 at all three locations. Filtered MeHg concentrations in the river showed no correlation to discharge or any other variable at Soapstone, Woodland, or Hailstone.

4. Discussion

www.manaraa.com

4.1 Mercury flushing from soils during snowmelt

Hg was flushed from soil during snowmelt and transported by ephemeral streams to the upper Provo River. The significant increase in THg concentrations seen on the log-log C-Q plot strongly suggests that Hg was mobilized during snowmelt events. The increase in THg concentrations (b>1) at Soapstone and Woodland below 20 m^3/s, followed by a decrease in concentrations (b<1), indicates that available THg was being flushed during the initial period of snowmelt. The log-log C-Q plot for Hailstone, which remained positive (b>1) through the entire range of discharge values, shows that THg concentrations increased and decreased proportionally to discharge during snowmelt.

Spatial differences in C-Q hysteresis loops observed in the upper Provo River are indicative of influences from different hydrologic mechanisms. At Soapstone and Woodland, clockwise hysteresis loop for filtered THg are the result of concentrations peaking on the rising limb of the hydrograph, and indicate that sources of Hg are proximal and well connected to the upper Provo River (Creed et al., 2015). Other studies in alpine environments have found C-Q patters of Hg similar to that of Soapstone and Woodland, and concluded that Hg was flushed from soils during the initial period of snowmelt (Mast et al., 2005). The clockwise figure-of-eight hysteresis loop observed at Hailstone is more complex, but still corresponds to a scenario where concentrations and discharge peak at similar times. A figure-of-eight hysteresis is produced by a combination of clockwise and counter-clockwise hysteresis patters (Williams, 1989). This combination could indicate that above Hailstone the river was possibly being diluted by water with distal and poorly connected sources of Hg.

Soil water is the primary source for THg in the upper Provo River during snowmelt. As snowmelt infiltrates and saturates soil, ephemeral streams are created, which transported Hg

www.manaraa.com

which was mobilized from soil. The concentrations of filtered THg in ephemeral streams is likely the result of DOM bound Hg flushed from soil (Grigal, 2002). Particulate Hg, which is typically associated with POM, is mobilized from the erosion of near surface soils (Bank, 2012a). The low fractions of particulate Hg in ephemeral streams could mean that there was minimal erosion of soils from snowmelt. High fractions of filtered THg at Soapstone indicate that ephemeral streams are the primary mechanism for transporting Hg to the upper Provo River. Although the Soapstone site had the closest proximity to active ephemeral streams, average filtered THg concentrations at Soapstone were slightly lower when compared to ephemeral streams. This decrease in filtered THg concentrations between ephemeral streams and Soapstone could be the result of dilution from baseflow or other sources of water such as the Duchesne diversion. Observed increases in the fraction of particulate THg at Woodland and Hailstone are possibly be the result of the resuspension of streambed sediments with bound Hg, or the in situ formation of particulate Hg from filtered THg (Grigal, 2002; Quémerais et al., 1999).

The majority of Hg in soils from the upper Provo River watershed is being retained during snowmelt. Using a report published from the USEPA, it is assumed that the primary source of Hg upper Provo River watershed is from atmospheric deposition (USEPA, 1997). Since we did not measure atmospheric Hg as part of this study, we assume that Hg deposition rates to the watershed are approximate to other locations with a similar climate in the western U.S. Using data from the National Atmospheric Deposition Program (NADP) annual Hg deposition rates were estimated at ~18 $\mu g/m^2$ (NADP, 2014). Using this deposition rate for the upper Provo River watershed (675 km^2), it was calculated that an Hg load of ~12 kg enters the upper Provo River watershed though wet deposition. With and average Hg flux of 1kg each year, this would indicate that ~92% of wet Hg deposition from the 2016 and 2017 water years was

www.manaraa.com

retained in soils. Dry deposition of Hg, which was not included in this study, can contribute just as much Hg to the terrestrial landscape as wet deposition (Mast et al., 2005). Therefore, it is likely that Hg deposition rates are underestimated, and that retention rates are even higher that 92%. The Hg load estimated from NADP rates are significantly higher than winter loads calculated from THg concentrations in snow. This could be due to Hg deposition rates being much higher during summer months because of the effects of insolation which increase the oxidation of Hg(0) in the atmosphere, and the greater effectiveness of rain in scavenging Hg compared to snow (Blackwell and Driscoll, 2015).

4.2 DOM characteristics and THg pathways during snowmelt

Changes in DOM characteristics during snowmelt indicted that DOM was originating from both microbial and terrestrial organic matter. In ephemeral streams, the most common species of DOM was from humic substances, and this was correlated to the changes seen in the river during snowmelt. Moderately high FI and BIX values during baseflow were indicative of microbial sourced organic matter and shifted more towards terrestrial plant and soil organic matter during snowmelt. This difference could be the result of changing microbial activity effecting DOM production during the snowmelt period (Malik and Gleixner, 2013). Changes in FI and BIX from Soapstone to Hailstone are indicative of microorganisms changing the properties of DOM during downstream transport (Cory and Kling, 2018). The previously established correlations between fDOM and filtered THg reinforces the argument that Hg transport was facilitated by fluorescent species of DOM such as humic and fulvic substances (Lescord et al., 2018). Binding of Hg to DOM is attributed to reduced sulfur sites in the organic matter, and is effected by characteristics such as pH and DOM source (Haitzer et al., 2003; Ravichandran, 2004). It has been observed that binding of Hg to certain types of DOM, such as

www.manaraa.com

humic acids, can be increased at pH ranges from 4-7(Haitzer et al., 2003). During the snowmelt period, the pH of soil water is often depressed to values below 7, and could trigger increased Hg-DOM binding.

4.3 Insight of high resolution filtered THg monitoring from in-situ fDOM measurements

The high correlation of filtered THg to in-situ fDOM (QSU) measurements allowed for the development of high resolution time-series data of filtered THg. This high-frequency filtered THg data can improve understanding of Hg fluxes in the upper Provo River as it has in other watersheds (Vermilyea et al., 2017). For example, it can be very difficult to obtain grab samples for THg during storm events, but through a proxy, THg concentrations and fluxes could be estimated during those events. The use of fDOM as a proxy to filtered THg is specific to the stream where THg concentrations were measured. Applying the Woodland proxy calculation to Hailstone would be problematic because unaccounted hydrologic influences, such as the Weber diversion, could complicate fDOM-THg relationships. The most significant problem with relying on fDOM as a proxy for filtered THg is the issue of equipment failure. During the 2016 and 2017 water years, there were large periods of time in which the fDOM sensors at Soapstone and Woodland did not record data, and would thus prevent the estimate of filtered THg concentrations.

4.4 Yearly filtered THg Loading at Jordanelle Reservoir

The upper Provo River contributes more to the total Hg load than atmospheric deposition onto the reservoir. The majority of water entering Jordanelle Reservoir is supplied from the upper Provo River. Given the fish consumption advisories in Jordanelle Reservoir due to elevated Hg concentrations in fish tissue, it is worth determining the amount of Hg inputs from

www.manaraa.com

the upper Provo River relative to atmospheric sources. The same Hg deposition rate of ~18 $\mu g/m^2$ for the upper Provo River watershed was used for Jordanelle Reservior. With a surface area of $1.2E^7$ m^2, this amounts to 0.22 kg of Hg deposition to the reservoir, which is only 22% of the Hg inputs from the river. Since the completion of Jordanelle Reservoir in April of 1993, assuming 1 kg/yr from the Provo River, approximately 30 kg of Hg have entered the reservoir by means of the river and atmospheric deposition. If these annual inputs of Hg to Jordanelle reservoir are accumulating in sediments, the availability of Hg for bioaccumulation could increase, potentially causing more issues with high Hg concentrations in fish tissue.

4.5 Lack of MeHg export during snowmelt

Filtered MeHg:filtered THg variability indicated that no significant amounts of filtered MeHg were exported during snowmelt. Although MeHg dynamics during snowmelt are poorly understood, saturation of soil from snowmelt is known to produce anoxic and low pH environments which can enhance MeHg production and export. MeHg, which has a high affinity to DOM (Klapstein and O'Driscoll, 2018), could be produced in soils and exported during snowmelt. However, no significant inputs of MeHg were seen to occur in the upper Provo River during snowmelt. It can thus be assumed that primary Hg methylation is occurring in the sediments of Jordanelle Reservior. In the study conducted by (Mast et al., 2005) similar MeHg concentrations were found in streams during snowmelt, and it was concluded that there were low net methylation rates in the watershed. The processes governing Hg methylation are complex and it is uncertain what factors are mitigating methylation in the soil of upper Provo River watershed. A more detailed study on spatial and temporal MeHg variably in the watershed would be necessary to quantify the impact of MeHg from soil water.

www.manaraa.com

5. Conclusion

This study of the upper Provo River watershed provides more insight to the understanding of Hg and DOM dynamics in montane watersheds. Atmospherically deposited Hg, which collected in soil, was flushed during snowmelt and caused THg concentrations to increase more than ten-fold in the upper Provo River. The load of Hg during the snowmelt period (typically April – July) accounted for ~90% of the total Hg flux each water year (2016 and 2017). Yearly loading of THg at Jordanelle Reservoir from the upper Provo River was estimated at ~ 1 kg with ~56% as filtered THg. THg transport was facilitated by DOM, primarily in the form of humic substances, which was originally sourced from shallow soils. Decreases in FI and BIX both spatially and temporally are indicative microbial influenced changes in DOM characteristics. The development of a filtered THg proxy through in situ fDOM (QSU) measurements provided a better understanding of Hg dynamics through high resolution filtered THg estimates. MeHg exported from upland soils was not significant for the total MeHg flux, and it can be assumed that MeHg production is primarily occurring in the reservoir. Additional research involving spatial and temporal Hg changes in watershed soils and Jordanelle Reservoir would add greatly to the understanding of Hg dynamics in this and similar watersheds.

www.manaraa.com

Table 1. Yearly and snowmelt runoff THg load comparisons at river sampling sites in the upper Provo River during the 2016 and 2017 water years.

Location	Water Year	Load (yearly)		Load (Snowmelt Runoff Period)		% Yearly THg load from snowmelt runoff
		Unfiltered THg (kg)	Filtered THg (kg)	Unfiltered THg (kg)	Filtered THg (kg)	
Soapstone	2016	0.66	0.49	0.64	0.48	97
Soapstone	2017	0.93	0.66	0.82	0.60	88
Woodland	2016	0.95	0.52	0.92	0.51	97
Woodland	2017	1.42	0.74	1.30	0.71	92
Hailstone	2016	0.80	0.54	0.70	0.47	86
Hailstone	2017	1.30	0.59	1.28	0.58	98

www.manaraa.com

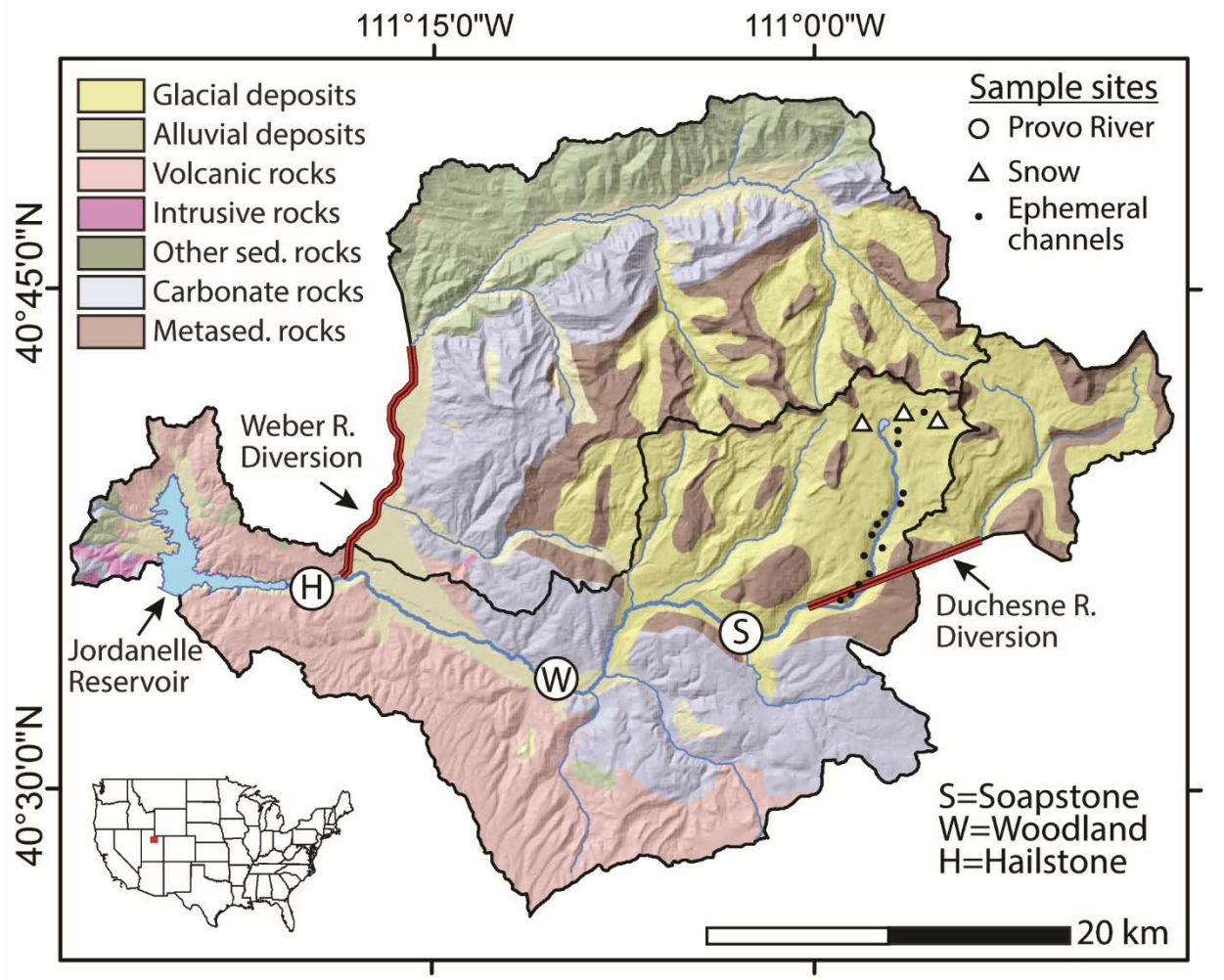

Figure 1. Simplified geologic map of the upper Provo River watershed (northern Utah, USA) showing sample locations, the Duchesne and Weber River diversions, and Jordanelle Reservoir.

www.manaraa.com

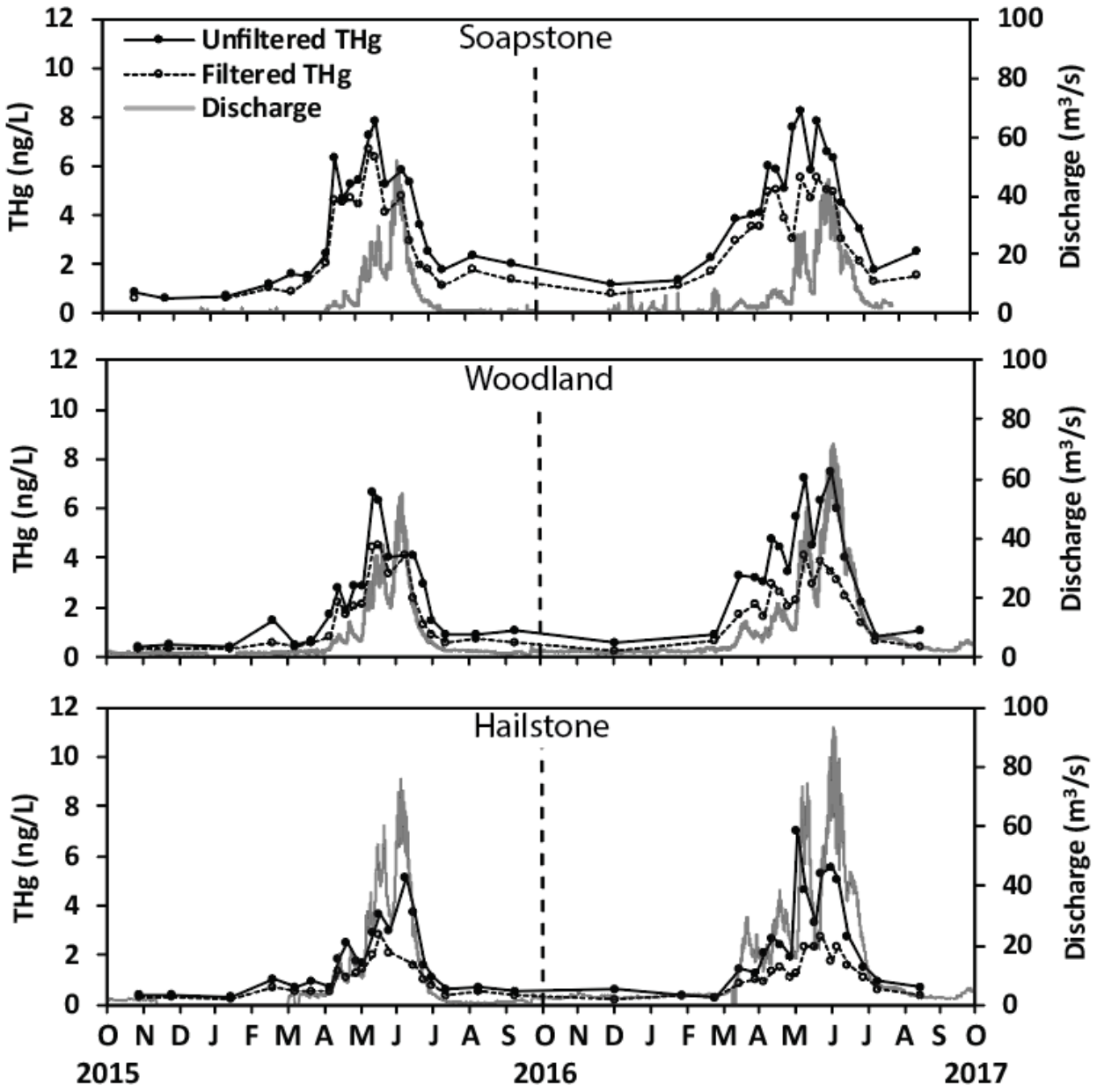

Figure 2. Discharge, total Hg, and filtered Hg at three sampling sites (Soapstone, Woodland, and Hailstone) in the Upper Provo River watershed. Runoff discharge is observable for two water years (2016 and 2017), with peak discharge occurring between late May and early June both years.

www.manaraa.com

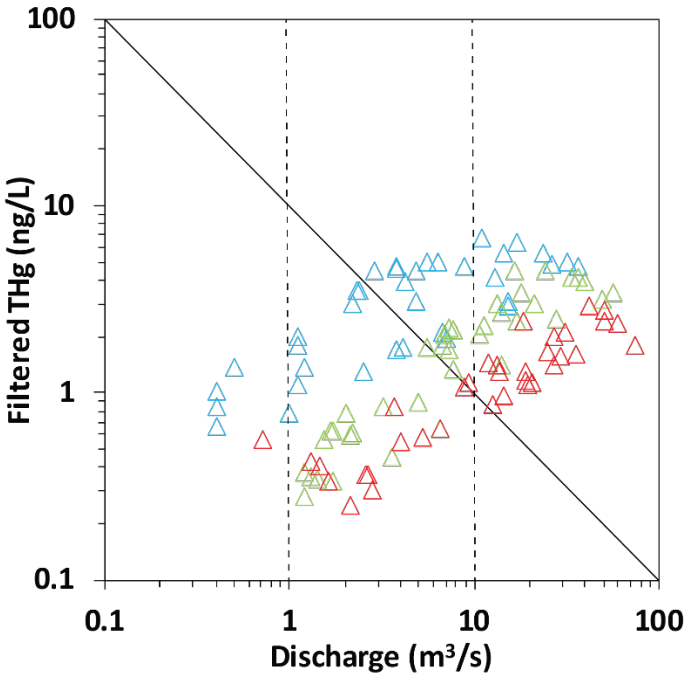

Figure 3. Log-Log C-Q plot for Soapstone (blue), Woodland (green), and Hailstone (red). Diagonal line from top left to bottom right represents a 1:1 dilution.

www.manaraa.com

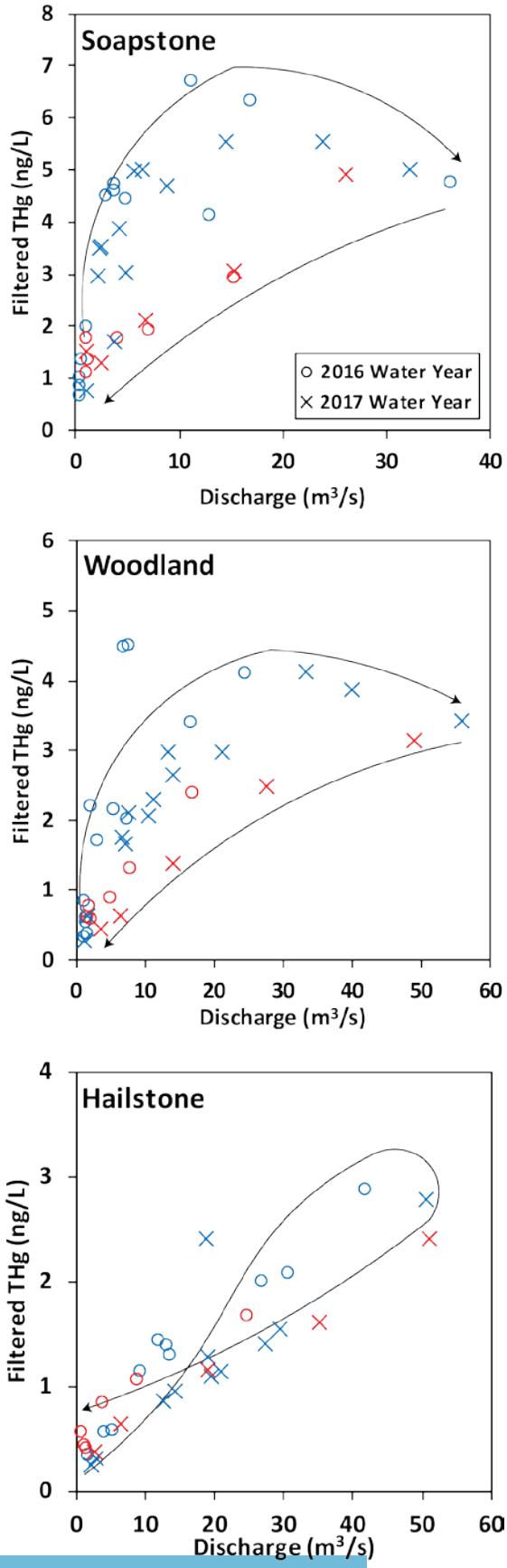

Figure 4. C-Q and Hysteresis loops for filtered THg at Soapstone, Woodland, and Hailstone during the 2016 and 2017 water years. The rising limb of the plot is in blue and the falling limb in red.

www.manaraa.com

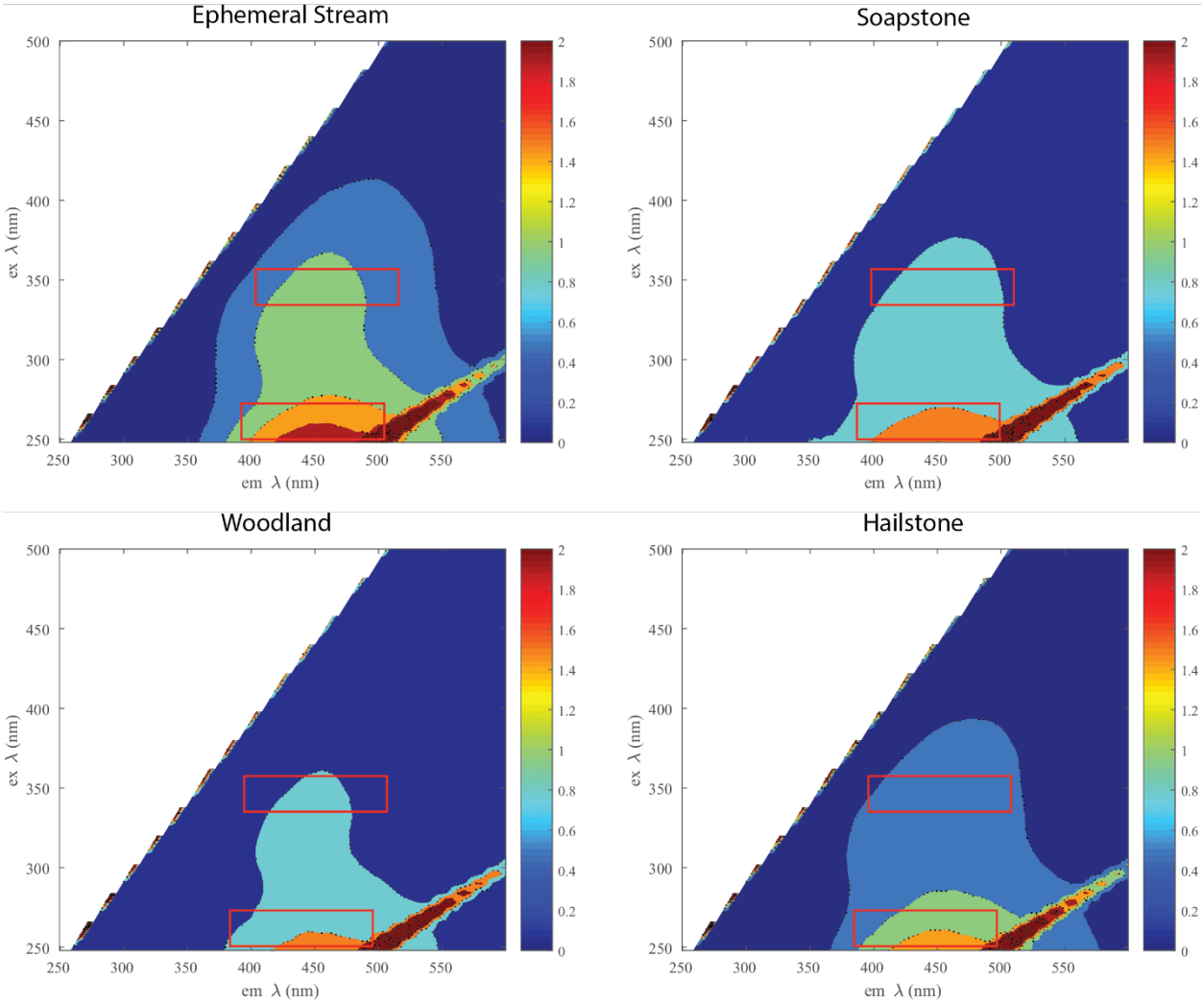

Figure 5. Excitation-emissions matrix (EEMs) for an ephemeral stream, Soapstone, Woodland, and Hailstone during snowmelt (May 2017). Red boxes indicate regions that correspond to humic substances.

www.manaraa.com

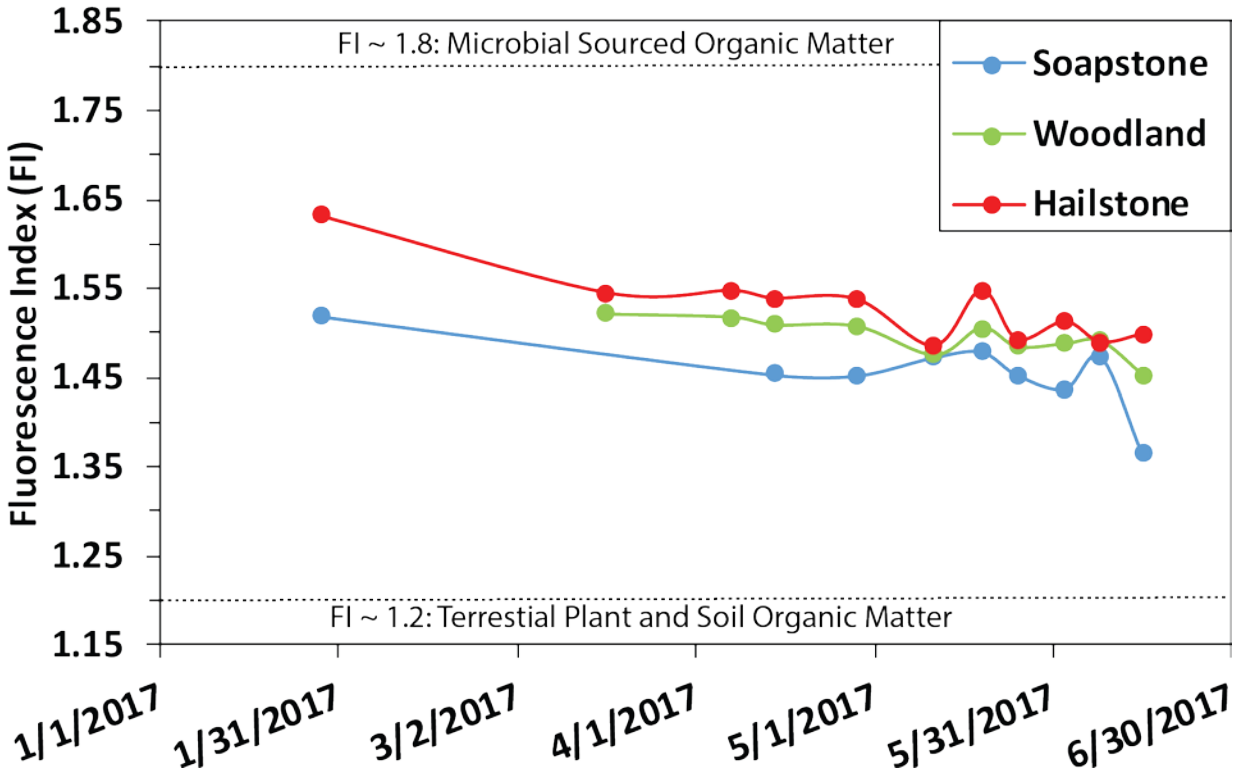

Figure 6. Fluorescence index (FI) at Soapstone, Woodland, and Hailstone during the 2017 water year. FI of all three sites decreases during snowmelt, indicating a greater input of terrestrial plant and soil organic matter.

www.manaraa.com

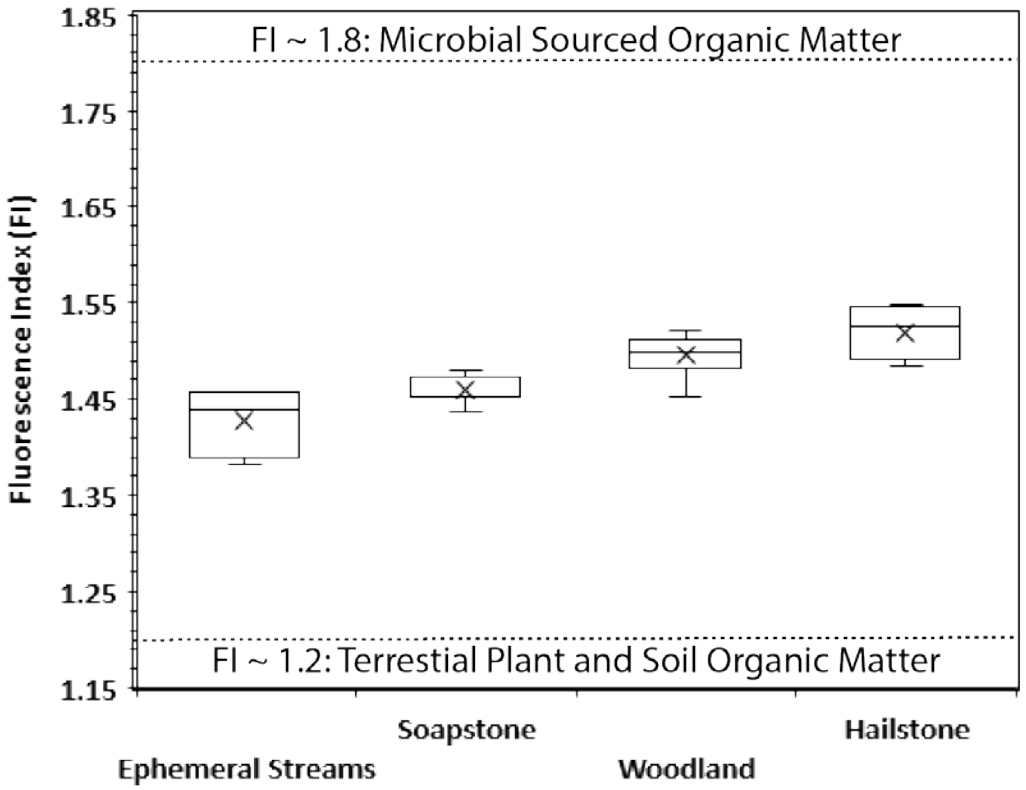

Figure 7. Fluorescence index (FI) of ephemeral streams and river sampling sites (Soapstone, Woodland, and Hailstone) during snowmelt (~ April-July). Ephemeral streams had the lowest FI indicating greater input from terrestrial plant and soil organic matter. FI increased downstream from Soapstone to Hailstone indicating a greater presence of microbial sourced organic matter.

www.manaraa.com

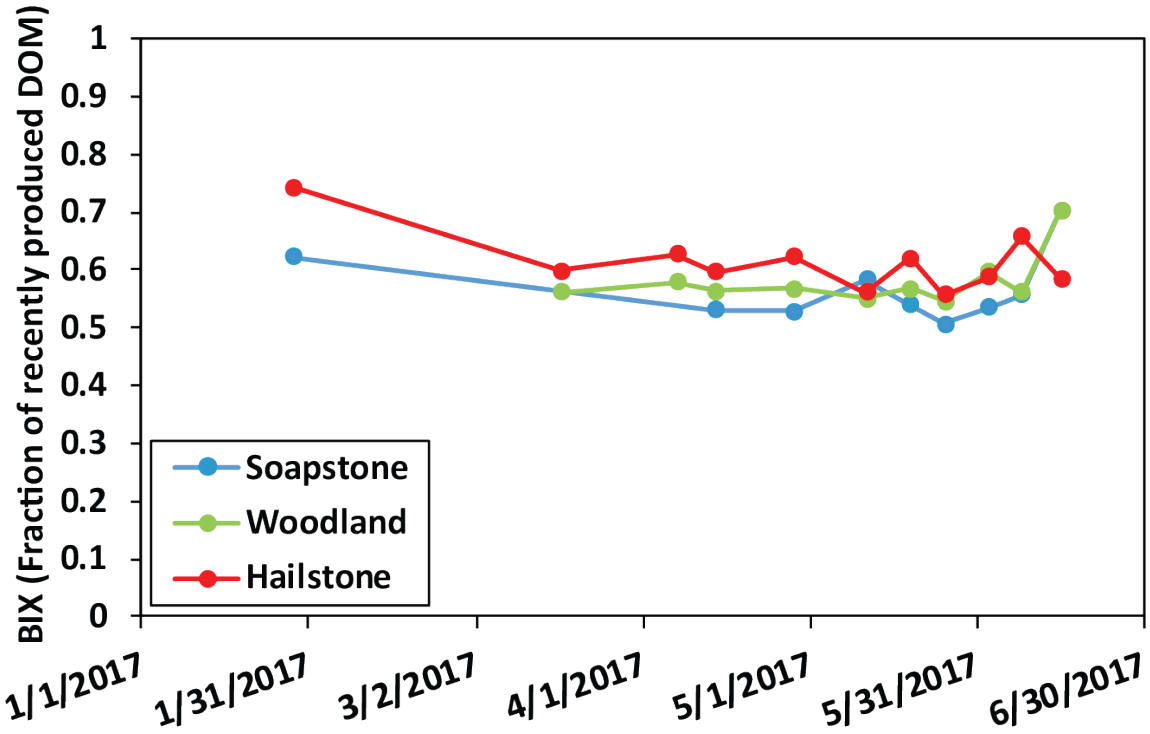

Figure 8. Freshness Index (BIX) at Soapstone, Woodland, and Hailstone during the 2017 water year. BIX of all three sites show a majority fraction of recently produced DOM (microbial) with slight decreases occurring between the months of March and June.

www.manaraa.com

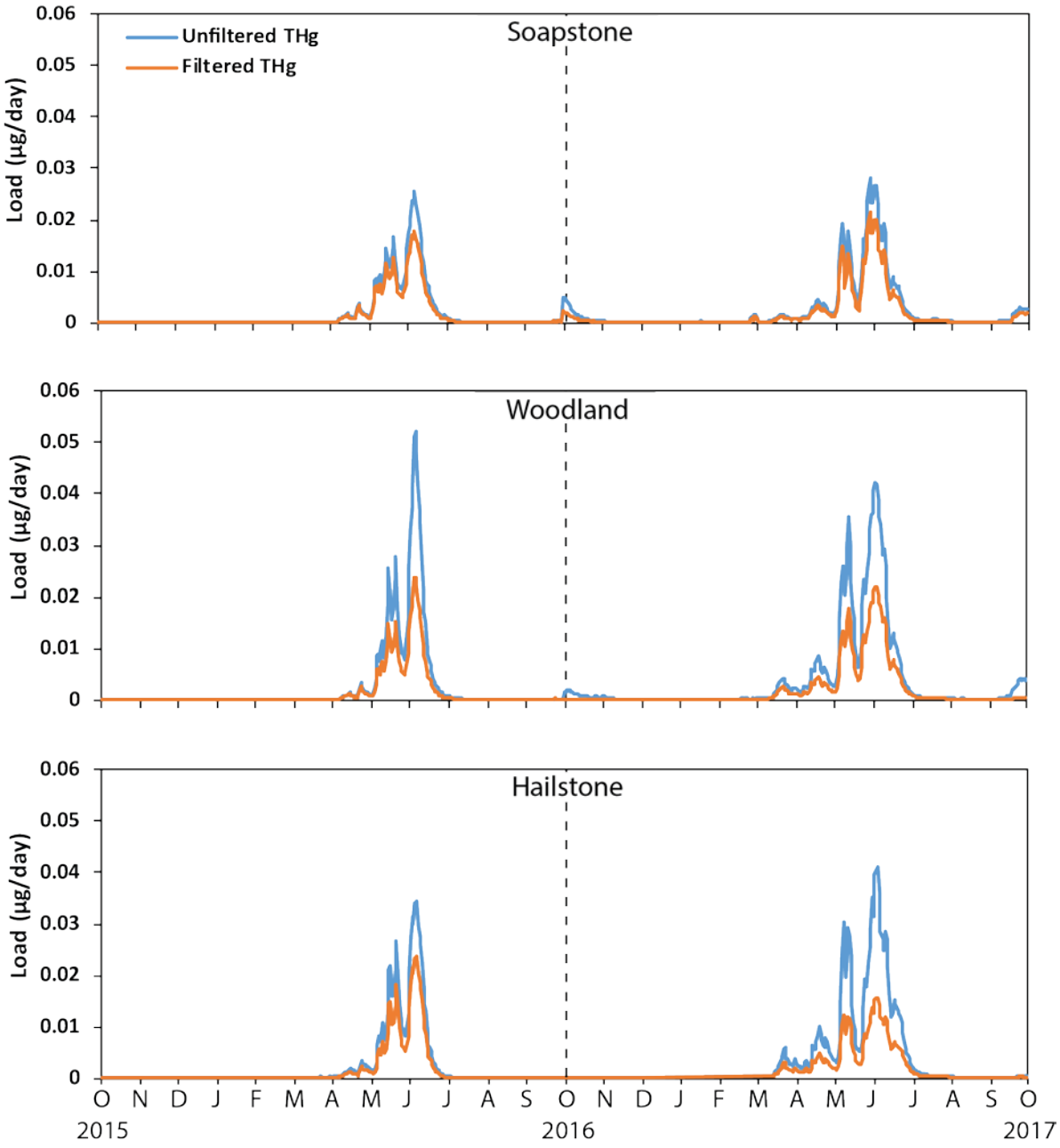

Figure 9. Daily filtered and unfiltered THg loads at Soapstone, Woodland and Hailstone for the 2016 and 2017 water years. The runoff period (early April - early July), contributed the majority (> 90%) of the THg load for the two water years.

www.manaraa.com

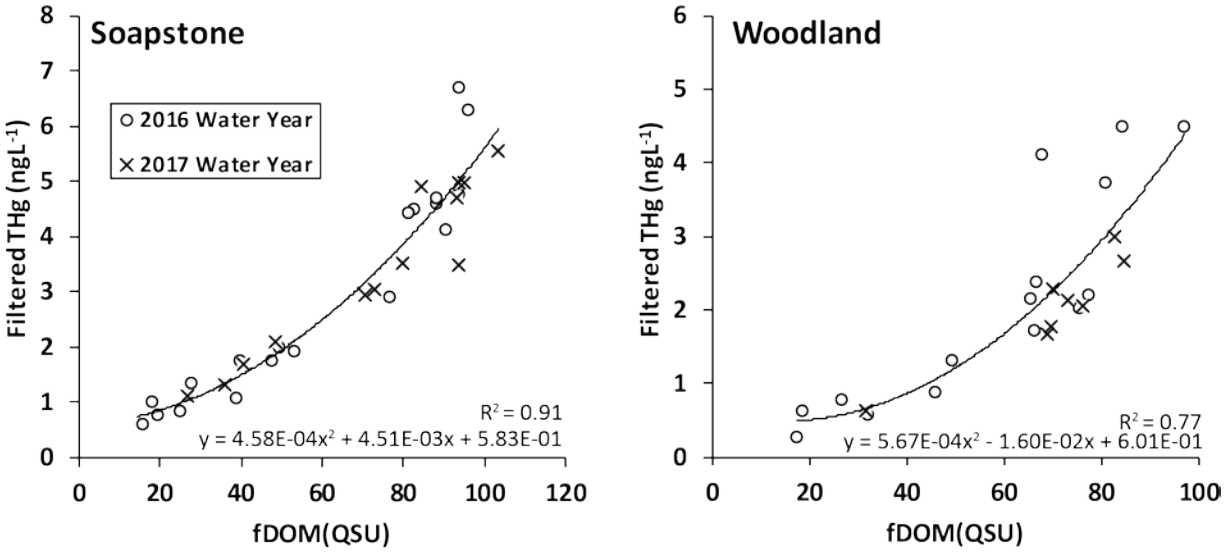

Figure 10. fDOM (QSU) vs filtered Hg at Soapstone and Woodland for the 2016 and 2017 water years. fDOM shows a strong correlation with filtered Hg at both locations. Polynomial equations for the two relationships were used to create a fDOM-fitlered THg proxy.

www.manaraa.com

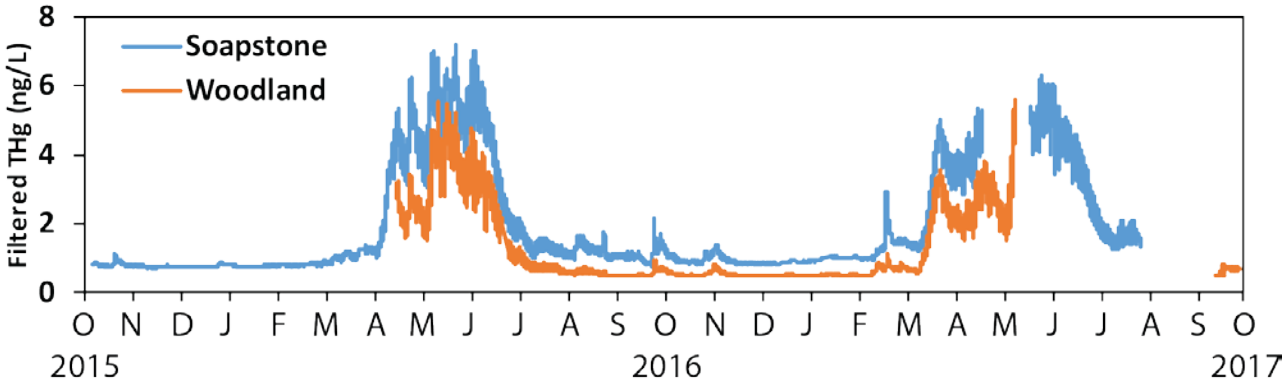

Figure 11. Calculated filtered THg from in-situ fDOM measurements at Soapstone and Woodland. Values across multiple periods missing due the fDOM sensor being offline.

www.manaraa.com

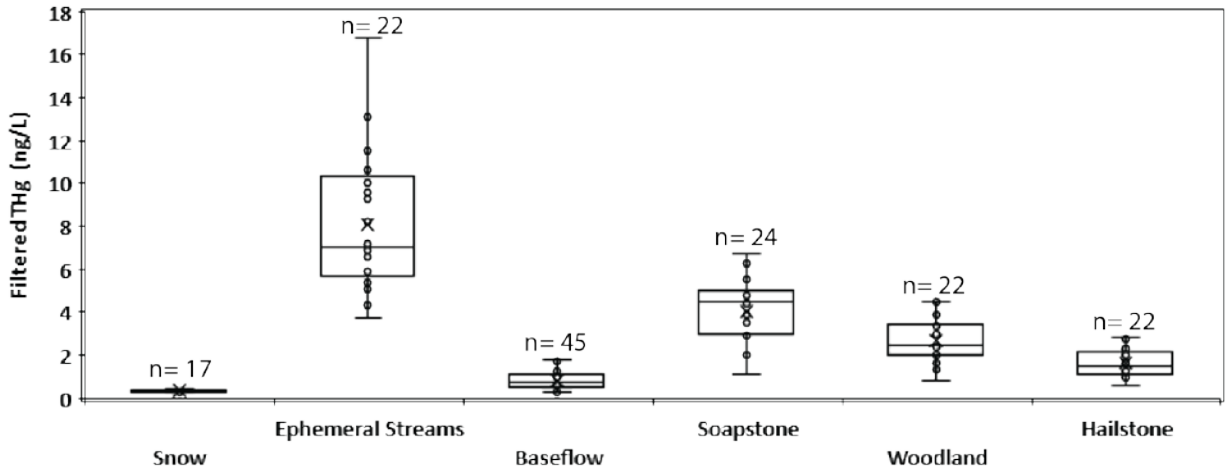

Figure 12. Concentration of filtered Hg of snow, ephemeral channels, baseflow, and river sampling sites (Soapstone, Woodland, and Hailstone). Each box plot contains concentration data from the 2016 and 2017 water years with total number of samples = n.

www.manaraa.com

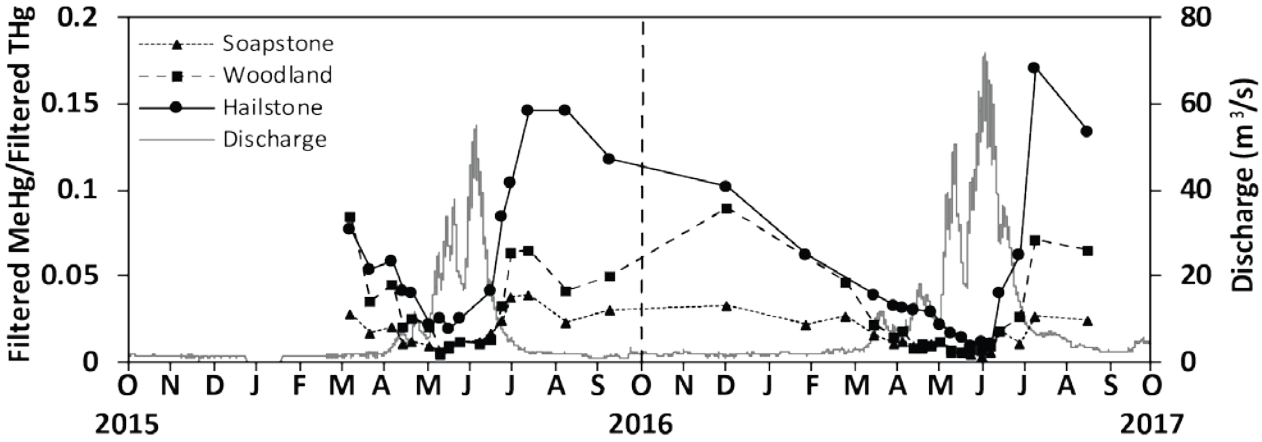

Figure 13. Filtered MeHg:filtered THg fraction Soapstone, Woodland, and Hailstone for the 2016 and 2017 water years. Filtred MeHg:filtered THg shows an inverse correlation with discharge at each site during both years.

www.manaraa.com

6. References

Bank MS. Mercury in the Environement: Patterns and Processes. In: Amirbahman A, Fernandez IJ, editors. Mercury in Terrestrial and Aquatic Environments. University of California Press, Los Angeles, CA, 2012a.

Bank MS. Mercury in the Evironment: Patterns and Processes. In: Shanley JB, editor. Mercury Cycling in Terrestrial Watersheds. 1. University of California Press, Los Angeles, CA, 2012b.

Bergamaschi BA, Krabbenhoft DP, Aiken GR, Patino E, Rumbold DG, Orem WH. Tidally Driven Export of Dissolved Organic Carbon, Total Mercury, and Methylmercury from a Mangrove-Dominated Estuary. Environmental Science & Technology 2012; 46: 1371-1378.

Blackwell BD, Driscoll CT. Deposition of Mercury in Forests along a Montane Elevation Gradient. Environmental Science & Technology 2015; 49: 5363-5370.

Carling GT, Fernandez DP, Johnson WP. Dust-mediated loading of trace and major elements to Wasatch Mountain snowpack. Science of The Total Environment 2012; 432: 65-77.

Chepyzhenko AI, Chepyzhenko AA. Methods and device for in situ dissolved organic matter (DOM) monitoring in natural waters' environment. XXIII International Symposium, Atmospheric and Ocean Optics, Atmospheric Physics. 10466. SPIE, 2017, pp. 5.

Cory RM, Kling GW. Interactions between sunlight and microorganisms influence dissolved organic matter degradation along the aquatic continuum. Limnology and Oceanography Letters 2018; 3: 102-116.

Creed IF, McKnight DM, Pellerin BA, Green MB, Bergamaschi BA, Aiken GR, et al. The river as a chemostat: fresh perspectives on dissolved organic matter flowing down the river continuum. Canadian Journal of Fisheries and Aquatic Sciences 2015; 72: 1272-1285.

Evans C, Davies TD. Causes of Concentration/Discharge Hyseresis and Its Potential as a Tool for Analysis of Episode Hydrochemistry. Vol 34, 1998.

Gabor R, Baker A, McKnight D, Miller M. Fluorescence indices and their interpretation, 2014.

Grigal DF. Inputs and outputs of mercury from terrestrial watersheds: a review. Environmental Reviews 2002; 10: 1-39.

Haitzer M, Aiken GR, Ryan JN. Binding of Mercury(II) to Aquatic Humic Substances: Influence of pH and Source of Humic Substances. Environmental Science & Technology 2003; 37: 2436-2441.

Haynes KM, Kane ES, Potvin L, Lilleskov EA, Kolka RK, Mitchell CPJ. Mobility and transport of mercury and methylmercury in peat as a function of changes in water table regime and plant functional groups. Global Biogeochemical Cycles 2017; 31: 233-244.

Klapstein SJ, O'Driscoll NJ. Methylmercury Biogeochemistry in Freshwater Ecosystems: A Review Focusing on DOM and Photodemethylation. Bulletin of Environmental Contamination and Toxicology 2018; 100: 14-25.

Lehnherr I, St. Louis VL, Emmerton CA, Barker JD, Kirk JL. Methylmercury Cycling in High Arctic Wetland Ponds: Sources and Sinks. Environmental Science & Technology 2012; 46: 10514-10522.

Lescord GL, Emilson EJS, Johnston TA, Branfireun BA, Gunn JM. Optical Properties of Dissolved Organic Matter and Their Relation to Mercury Concentrations in Water and Biota Across a Remote Freshwater Drainage Basin. Environmental Science & Technology 2018; 52: 3344-3353.

Lowry JH, Ramsey RD, Boykin D, Bradford P, Comer S, Falzarano W, et al. Southwest Regional Gap Analysis Project: Final Report on Land Cover Mapping Methods. RS/GIS Laboratory, Utah State University, Logan, Utah, 2005.

Lu X, Jaffe R. Interaction between Hg(II) and natural dissolved organic matter: a fluorescence spectroscopy based study. Water Research 2001; 35: 1793-1803.

Lucotte M, Mucci A, Killaire-Marcel C, Pichet P, Grondin A. Anthropogenic Mercury Enrichment in Remote Lakes of Northern Québec (Canada). In: Porcella DB, Huckabee JW, Wheatley B, editors.

www.manaraa.com

Mercury as a Global Pollutant: Proceedings of the Third International Conference held in Whistler, British Columbia, July 10–14, 1994. Springer Netherlands, Dordrecht, 1995, pp. 467-476.
Malik A, Gleixner G. Importance of microbial soil organic matter processing in dissolved organic carbon production. FEMS Microbiology Ecology 2013; 86: 139-148.
Mansfield CR, Black FJ. Quantification of monomethylmercury in natural waters by direct ethylation: Interference characterization and method optimization. Limnology and Oceanography: Methods 2015; 13: e10009.
Mast MA, Campbell DH, Krabbenhoft DP, Taylor HE. Mercury Transport in a High-Elevation Watershed in Rocky Mountain National Park, Colorado. Water, Air, and Soil Pollution 2005; 164: 21-42.
Mergler D, Anderson HA, Laurie Hing Man C, Mahaffey KR, Murray M, Mineshi S, et al. Methylmercury Exposure and Health Effects in Humans: A Worldwide Concern. Ambio 2007; 36: 3-11.
Morel FMM, Kraepiel AML, Amyot M. The chemical cycle and bioaccumulation of mercury. Annual Review of Ecology and Systematics 1998; 29: 543-566.
Munroe JS. Physical, Chemical, and Thermal Properties of Soils across a Forest-Meadow Ecotone in the Uinta Mountains, Northeastern Utah, U.S.A. Arctic, Antarctic, and Alpine Research 2012; 44: 95-106.
NADP. Total Mercury Wet Deposition, 2014. National Atmospheric Deposition Program/Mercury Deposition Network, Champaign, IL, 2014.
Paranjape AR, Hall BD. Recent advances in the study of mercury methylation in aquatic systems. FACETS 2017; 2: 85-119.
Quémerais B, Cossa D, Rondeau B, Pham TT, Gagnon P. Sources and Fluxes of Mercury in the St. Lawrence River. Environmental Science & Technology 1999; 33: 840-849.
Ravichandran M. Interactions between mercury and dissolved organic matter--a review. Chemosphere 2004; 55: 319-31.
Rue GP, Rock ND, Gabor RS, Pitlick J, Tfaily M, McKnight DM. Concentration-discharge relationships during an extreme event: Contrasting behavior of solutes and changes to chemical quality of dissolved organic material in the Boulder Creek Watershed during the September 2013 flood. Water Resources Research 2017; 53: 5276-5297.
Runkel R, Crawford C, Cohn T. Load estimator (LOADEST): a FORTRAN program for estimating constituent loads in streams and rivers, 2004.
Schroeder WH, Munthe J. Atmospheric mercury—An overview. Atmospheric Environment 1998; 32: 809-822.
Stedmon CA, Bro R. Characterizing dissolved organic matter fluorescence with parallel factor analysis: a tutorial. Limnology and Oceanography: Methods 2008; 6: 572-579.
Streets DG, Devane MK, Lu Z, Bond TC, Sunderland EM, Jacob DJ. All-Time Releases of Mercury to the Atmosphere from Human Activities. Environmental Science & Technology 2011; 45: 10485-10491.
Ullrich SM, Tanton TW, Abdrashitova SA. Mercury in the aquatic environment: A review of factors affecting methylation. Critical Reviews in Environmental Science and Technology 2001; 31: 241-293.
USEPA. Method 1669: Sampling Ambient Water for Trace Metals at EPA Water Quality Criteria Levels : Draft: U.S. Environmental Protection Agency, Office of Water, 1996.
USEPA. Mercury Study Report to Congress. In: Agency USEP, editor. EPA-452-97-003. Office of Air and Radiation, Washington, D.C., 1997.
USEPA. EPA Method 1631, Revision E: Mercury in Water by Oxidation , Purge and Trap, and Cold Vapor Atomic Fluorescence. Revision E. US Environmental Protection Agency, Washinton D.C., 2002, pp. 38 pp.

www.manaraa.com

Vermilyea AW, Nagorski SA, Lamborg CH, Hood EW, Scott D, Swarr GJ. Continuous proxy measurements reveal large mercury fluxes from glacial and forested watersheds in Alaska. Science of The Total Environment 2017; 599-600: 145-155.

Williams GP. Sediment concentration versus water discharge during single hydrologic events in rivers. Journal of Hydrology 1989; 111: 89-106.

Winnick MJ, Carroll RWH, Williams KH, Maxwell RM, Dong W, Maher K. Snowmelt controls on concentration-discharge relationships and the balance of oxidative and acid-base weathering fluxes in an alpine catchment, East River, Colorado. Water Resources Research 2017; 53: 2507-2523.

Woods AJ, Lammers DA, Bryce SA, Omernik JM, Denton RL, Domeier M, et al. Ecoregions of Utah (color poster with map, descriptive text, summary tables, and photographs). U.S. Geological Survey, Reston, Viginia, 2001.

Xie W, Zhang S, Ruan L, Yang M, Shi W, Zhang H, et al. Evaluating Soil Dissolved Organic Matter Extraction Using Three-Dimensional Excitation-Emission Matrix Fluorescence Spectroscopy. Pedosphere 2017; 27: 968-973.

www.manaraa.com